

ARTICLE

IMPROVEMENT OF AUTOMATIC HEMORRHAGES DETECTION METHODS IN RETINAL IMAGING AND IMAGE ANALYSIS

M Anto Bennet^{1*}, J Surekha Poomathi², C Kalpana³, S Sariga Priya⁴

¹Professor, ^{2,3,4}UG Students, Department of ECE, VEL TECH, Avadi, Chennai 600 062, Tamil Nadu, INDIA

ABSTRACT

Our vision reduced in eye due to the presence of Retinal diseases like Exudates (diabetic Retinopathy), Micro aneurysms, and Blood vessel damage. This work mainly concentrates on the symptoms of heart, lung, liver and kidney problems identification using Retinal fundus images. Our proposed work shows that how optic disk elimination and follower the symptom detection. Optic disk is one of the parts which consist of intersection of blood vessels and it also has same characteristics of exudates like yellow color, intensity and contrast. Distinguish the exudates and optic disk is critical one. So only first eliminate the optic disk and follower that exudates detection. This detection method very favorably with existing and promise deployment of these systems. Micro aneurysms are the initial stage of exudates.

INTRODUCTION

Hemorrhage is defined as an escape of blood from ruptured blood vessel. Ischemia is a term used to describe a tissue whose blood supply has been reduced to an insufficient level. Lack of O₂ in the retinal tissue may lead to retinal cell death and result in reduced vision shown in [Fig. 1].

The problems in kidney and Lung are detected through Micro aneurysm formation in Retina. The kidneys are bean shaped organs that serve several essential regulatory roles in vertebrate animals [1]. They are essential in the urinary system and also serve homeostatic functions such as the regulation of electrolytes, maintenance of acid-base balance, and regulation of blood pressure (via maintaining salt and water balance). They serve the body as a natural filter of the blood, and remove wastes, which are diverted to the urinary bladder. In producing urine, the kidneys excrete wastes such as urea and ammonium, and they are also responsible for the reabsorption of water, glucose, and amino acids. The kidneys also produce hormones including calcitriol, erythropoietin, and the enzyme rennin. Located at the rear of the abdominal cavity in the retroperitoneal, the kidneys receive blood from the paired renal arteries, and drain into the paired renal veins. Each kidney excretes urine into a urethra, itself a paired structure that empties into the urinary bladder. Renal physiology is the study of kidney function, while nephrology is the medical specialty concerned with kidney diseases. Diseases of the kidney are diverse, but individuals with kidney disease frequently display characteristic clinical features. Common clinical conditions involving the kidney include the nephritic and nephrotic syndromes, renal cysts, acute kidney injury, chronic kidney disease, urinary tract infection, nephrolithiasis, and urinary tract obstruction. Various cancers of the kidney exist; the most common adult renal cancer is renal cell carcinoma [2,3]. Cancers, cysts, and some other renal conditions can be managed with removal of the kidney, or nephrectomy. When renal function, measured by lomerular filtration rate, is persistently poor, dialysis and kidney transplantation may be treatment options. Although they are not normally harmful, kidney stones can be painful and repeated, chronic formation of stones can scar the kidneys. The removal of kidney stones involves ultrasound treatment to break up the stones into smaller pieces, which are then passed through the urinary tract. One common symptom of kidney stones is a sharp to disabling pain in the medial/lateral segments of the lower back or groin shown in [Fig. 2].

KEY WORDS

Adaptive Histogram Equalization (AHE), Gray-Level Co-occurrence Matrix (GLCM), Contrast limited AHE (CLAHE).

Received: 24 October 2016
Accepted: 20 December 2016
Published: 15 February 2017

*Corresponding Author
Email:
bennetmab@gmail.com



Fig. 1: Retina with hemorrhage formation

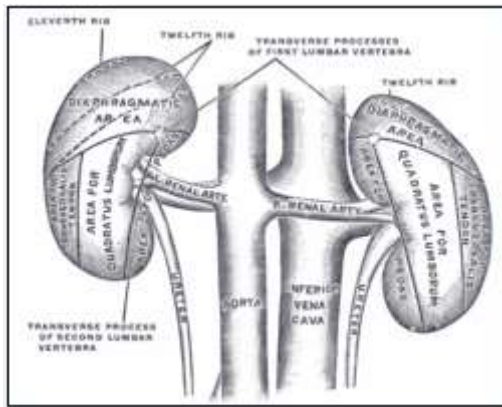


Fig. 2: Diagram of Kidney

3D-rendered computed tomography, showing renal arteries and veins. The kidneys receive blood from the renal arteries, left and right, which branch directly from the abdominal aorta. Despite their relatively small size, the kidneys receive approximately 20% of the cardiac output [4]. Each renal artery branches into segmental arteries, dividing further into interlobar arteries, which penetrate the renal capsule and extend through the renal columns between the renal pyramids. The interlobar arteries then supply blood to the arcuate arteries that run through the boundary of the cortex and the medulla. Each arcuate artery supplies several interlobular arteries that feed into the afferent arterioles that supply the glomeruli. The medullary interstitium is the functional space in the kidney beneath the individual filters (glomeruli), which are rich in blood vessels [5,6]. The interstitium absorbs fluid recovered from urine. Various conditions can lead to scarring and congestion of this area, which can cause kidney dysfunction and failure. After filtration occurs the blood moves through a small network of venules that converge into interlobular veins. As with the arteriole distribution the veins follow the same pattern, the interlobular provide blood to the arcuate veins then back to the interlobar veins, which come to form the renal vein exiting the kidney for transfusion for blood. The kidney participates in whole-body homeostasis, regulating acid-base balance, electrolyte concentrations, extracellular fluid volume, and regulation of blood pressure. The kidney accomplishes these homeostatic functions both independently and in concert with other organs, particularly those of the endocrine system. Various endocrine hormones coordinate these endocrine functions; these include renin, angiotensin II, aldosterone, antidiuretic hormone, and atrial natriuretic peptide, among others. Many of the kidney's functions are accomplished by relatively simple mechanisms of filtration, reabsorption, and secretion, which take place in the nephron [7]. Filtration, which takes place at the renal corpuscle, is the process by which cells and large proteins are filtered from the blood to make an ultrafiltrate that eventually becomes urine. The kidney generates 180 liters of filtrate a day, while reabsorbing a large percentage, allowing for the generation of only approximately 2 liters of urine. Reabsorption is the transport of molecules from this ultrafiltrate and into the blood. Secretion is the reverse process, in which molecules are transported in the opposite direction, from the blood into the urine. Although the kidney cannot directly sense blood, long-term regulation of blood pressure predominantly depends upon the kidney. This primarily occurs through maintenance of the extracellular fluid compartment, the size of which depends on the plasma sodium concentration. Renin is the first in a series of important chemical messengers that make up the renin-angiotensin system [8]. Changes in renin ultimately alter the output of this system, principally the hormones angiotensin II and aldosterone. Each hormone acts via multiple mechanisms, but both increase the kidney's absorption of sodium chloride, thereby expanding the extracellular fluid compartment and raising blood pressure. When renin levels are elevated, the concentrations of angiotensin II and aldosterone increase, leading to increased sodium chloride reabsorption, expansion of the extracellular fluid compartment, and an increase in blood pressure. Conversely, when renin levels are low, angiotensin II and aldosterone levels decrease, contracting the extracellular fluid compartment, and decreasing blood pressure [9].

MATERIALS AND METHODS

The Retinal fundus images are converted to either green component or gray scale for feature extraction. The green channel extractions are then fed into image enhancement. Low contrast images could often due to several reasons, such as poor (or) non uniform lightning condition, non-linearity (or) small dynamic range of image sensor. Image enhancement features are then fed into morphological dilation, erosion and opening operation. Dilation is used for expanding an element. Erosion is used for shrinking an element. And opening operation is used to remove a optical disk using radius formula. The circular border is then fed into pixel classification. In pixel classification uses a techniques namely Graycoprops. Graycoprops normalizes the gray-level co-occurrence matrix (GLCM) so that the sum of its elements is equal to 1. There are four techniques are used to classify the GLCM are contrast, correlation, homogeneity and energy. The

input image operation is performed using mat lab syntax. Finally, the output images (i.e.,) Blood Vessels, micro-aneurysm and exudates are obtained shown in [Fig. 3].

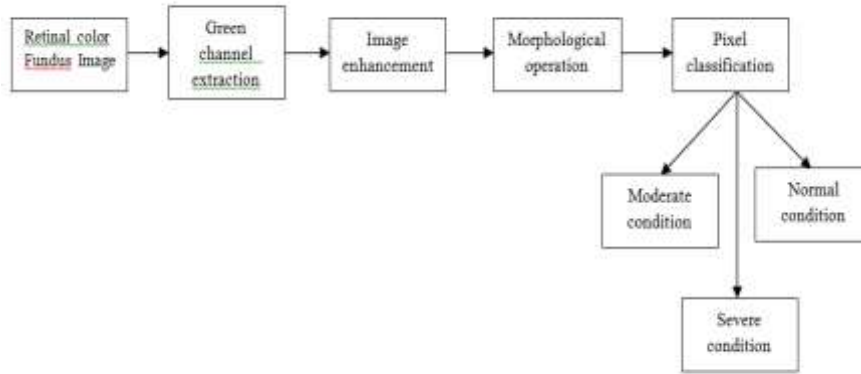


Fig. 3: Block diagram of automatic hemorrhages detection method

RETINAL COLOR FUNDUS IMAGES

The color retinal images are taken using fundus camera. It consists of three colors red, green, and blue. Since background of retina is red in color we omit red color in the image and blue color have high wavelength of noise and it is omitted and we take only green channel in the image shown in [Fig. 4].

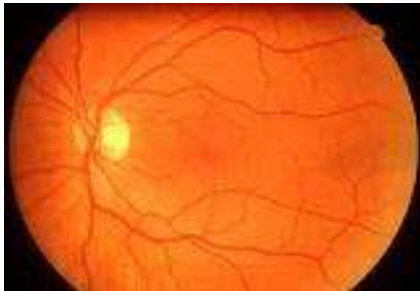


Fig. 4: Color fundus image

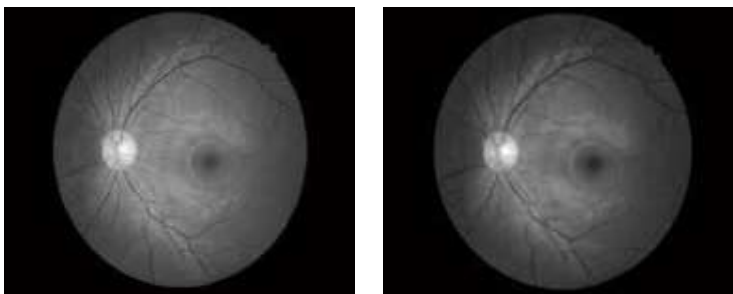


Fig. 5: Green channel extraction and gray scale image.

GREEN CHANNEL EXTRACTION

The color fundus images are converted to either green component or grayscale for features extraction of texture analysis. Green channel provides maximum contrast between background and foreground shown in [Fig. 5].

IMAGE ENHANCEMENT

The normalized features values are then fed into image enhancement. Low contrast images could often be due to several reasons, such as poor (or) non uniform lighting condition, non-linearity (or) small dynamic range of image sensor.

ADAPTIVE HISTOGRAM EQUALIZATION

Adaptive Histogram Equalization (AHE) is a computer image processing technique used to improve contrast in images. It differs from ordinary histogram equalization in the respect that the adaptive method computes several histograms, each corresponding to a distinct section of the image, and uses them to redistribute the lightness values of the image. It is therefore suitable for improving the local contrast of an image and bringing out more detail. However, AHE has a tendency to over amplify noise in relatively homogeneous regions of an image shown in [Fig. 6].

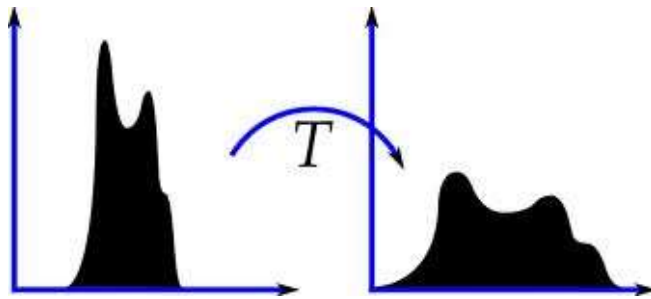


Fig. 6: Adaptive Histogram Equalization

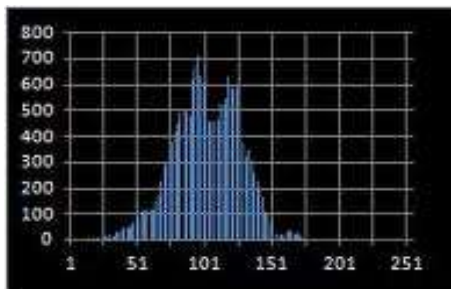


Fig. 7: Real Time Performance of AHE

Experience has shown that the size of the contextual region can be set to either $1/16$ or $1/64$ of the image area for essentially all medical images, with the smaller region chosen only when the feature size of interest is quite small. With a smaller contextual region the contrast becomes too sensitive to very local variations and in particular to image noise. The oversensitivity to local variations can cause artifacts, which have never been experienced with the preferred contextual region sizes. Although AHE frequently produces excellent result in certain cases noise becomes disturbingly obvious. In particular, this occurs where the image includes relatively homogeneous regions or a poor signal to noise ratio [Fig. 7]. Contrast limited AHE (CLAHE) avoids this over enhancement of noise. Contrast enhancement can be defined as the slope of the function mapping input intensity to output intensity. We will assume that the range of input and output intensities is the same. Then a slope of 1 involves no enhancement, and higher slopes give increasingly higher enhancement. Thus the limitation of contrast enhancement can be taken to involve restricting the slope of the mapping function. With histogram equalization the mapping function $m(i)$ is proportional to the cumulative Histogram:

$$m(i) = (\text{Display-Range}) \cdot (\text{Cumulative_Histogram}(i) / \text{Region-Size}) \quad (1)$$

Since the derivative of the cumulative histogram is the histogram, the slope of the mapping function at any input intensity, i.e. the contrast enhancement, is proportional to the height of the histogram at that intensity: $dm/di = (\text{Display-Range} / \text{Region-Size}) \cdot \text{histogram}(i)$. Therefore limiting the slope of the mapping function is equivalent to clipping the height of the histogram shown in [Fig. 8].

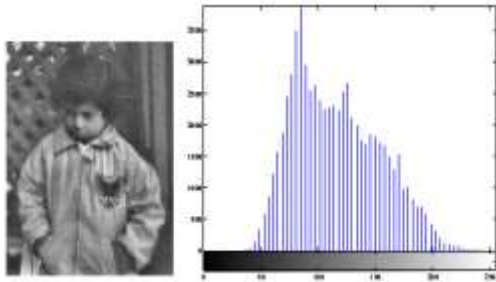


Fig. 8: Image after CLAHE equalization with its histogram .

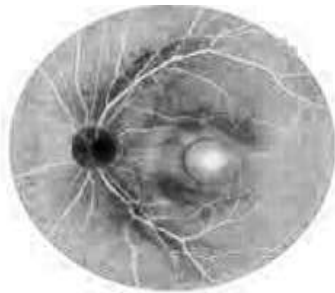


Fig. 9: Image and histogram after adaptive histogram equalization

CLAHE operates on small regions in the image, called tiles, rather than the entire image. Each tile's contrast is enhanced, so that the histogram of the output region approximately matches the histogram specified by the 'Distribution' parameter. The neighboring tiles are then combined using bilinear interpolation to eliminate artificially induced boundaries. The contrast, especially in homogeneous areas, can be limited to avoid amplifying any noise that might be present in the image shown in [Fig. 9].

MORPHOLOGICAL OPERATION

Based on shapes input size is equal to the output size. The each pixel in output image is compared to corresponding pixel in the input image with its neighbors.

Detection of retinal vessels

The input retinal images are first to be detected for abnormal vessels in the retinal region. Studies show that earlier techniques such as the holding and histogram equalization have shown cases of missing out thin vessels which is a serious problem. The main reason behind is the resultant image obtained via the techniques implemented previously were blurred with lack of accuracy. The proposed methodology aimed at performing the curve let transform for effective enhancement of the image for better viewing along with effective edge detection using the multi structure morphological reconstruction for detecting the edges along eight directionalities unlike mathematical morphology

Dilation

Dilation is used for expanding an element A by using structuring element B. Dilation of A by B and is defined by the following equation:

$$A \oplus B = \{z \mid (B)_z \cap A \neq \emptyset\} \tag{2}$$

This equation is based on obtaining the reflection of B about its origin and shifting this reflection by z. The dilation of A by B is the set of all displacements z, such that A and B overlap by at least one element.

Based On this interpretation the equation of can be rewritten as:

$$A \oplus B = \{Z \mid [(B)Z \cap A] \subset A\} \tag{3}$$

Erosion

Erosion is used for shrinking of element A by using element B. Erosion for Sets A and B in Z^2 , is defined by the Following equation:

$$A \oplus B = \{z | [(B)_z \cap A] \subset A\} \quad (4)$$

This equation indicates that the erosion of A by B is the set of all points z such that B, translated by z, is combined in A shown in [fig 10&11].



Fig. 10: Output of erosion and dilation of an image

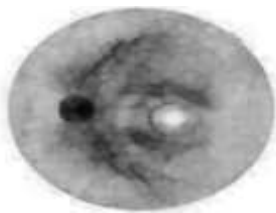


Fig.11: Image after imerode and indilate

FEATURE EXTRACTION

Different features of the fundus images namely Blood vessels, Exudates and Micro aneurysms are extracted using image processing techniques. The values obtained are essential as they represent the image and are necessary in order to classify the images accurately.

EXPERIMENTAL PROCEDURE FOR BORDER FORMATION

There are two methods in detecting the circular border of an image. Both methods are essential as each method could not work for few of the images due to their contrast intensity. Deploying both methods allow the detection of all the images. Border formation is to clean off the noisy edges and is also use during exudates, micro aneurysm and blood vessel.

Border formation method 1

Grayscale image instead of green channel is used as it more efficient for border formation. The first method uses canny method to detect the edges before enclosing the circular region with a top and bottom bar. Function “imfill” is then applied to fill the region. The circular border is then formed by subtracting the eroded and dilated images shown in [Fig 12].

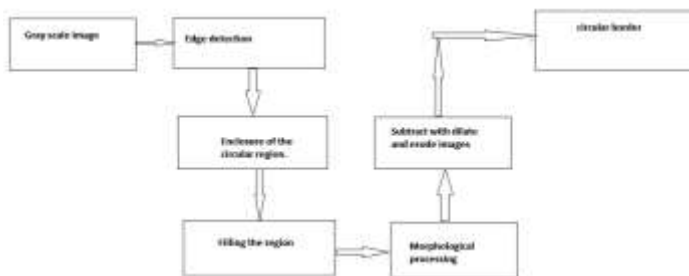


Fig. 12: border formation method 1

Border formation method 2

Method 2 is activated when a noisy image is obtained instead of a circular border. This method inverses the intensity of the images first before image segmentation is applied with function. The circular region is filled as a result and the circular border obtained after subtracting the dilated image with eroded image shown in [Fig. 13 &14].

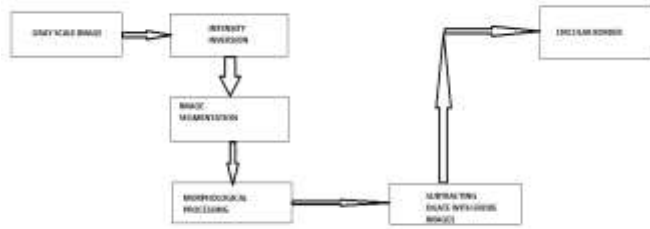


Fig. 13: Border formation method 2

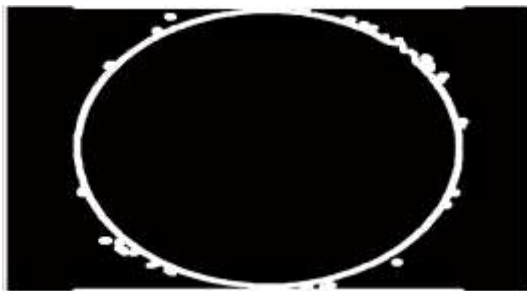


Fig.14: Subtracted image.

EXPERIMENTAL PROCEDURE-MASK OPERATION FOR OPTIC DISK

As optic disk is made up of a group of bright spots, it is not suitable to use loops and locate the largest value. This would only point to one spot and most likely to be on the side of optical disk. The mask required to cover optical disk would be inefficient as it would be much larger and covers more details. Mask creation is used in the detection of blood vessels, exudates and micro aneurysm. After locating the optic disk, a mask needed to be created. A simple mask created using loops would be easy but it would be result in error when the optic disk is close to the image shown in [Fig. 15& 16].

$$P2=(x-k)^2+(y-h)^2 \quad (5)$$

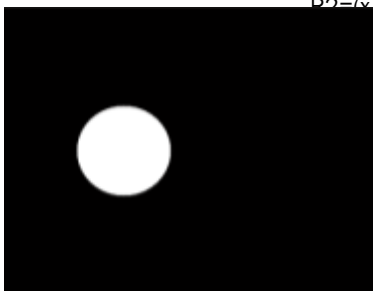


Fig. 15: Removal of optic disk.



Fig. 16: Image after removal of optic disk

EXPERIMENTAL PROCEDURE-AND LOGIC

Two methods of detecting blood vessels are used. Both methods generally detect different location of the images like exudates as blood vessels; hence by computing their similarity the non blood vessels area could be filtered. AND logic is applied to mark out the similar pixels of the two images. The output pixel is registered as binary1 (white) when both images' pixels are binary1(white) the obtained image would be clearer shown in [Fig. 17&18].



Fig.17: Blood vessel with Noise & mask



Fig.18: Blood vessel & noise after adaptive histogram

RESULT

The area of blood vessel is obtained using two loops to count the number of pixels with binary 1(white) in the final blood vessel image shown in [Fig.19]. Finally the corresponding values are shown in [Table 1].

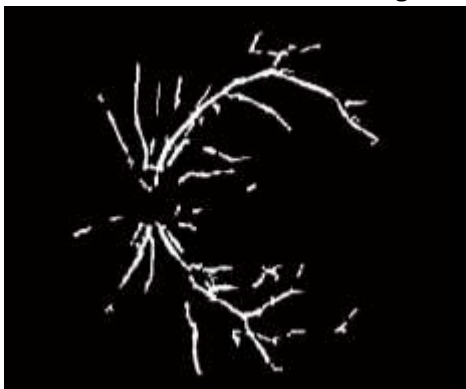


Fig.19: Final blood vessel image

Table 1. Threshold Values For Blood Vessels

AREA	ENERGY	CONTRAST	CORRELATION	HOMOGENITY	OUTPUT
15435	0.269534	0.941772713	0.121151769	0.871993035	0
14176	0.270413	0.936932181	0.123631065	0.871076244	0
17575	0.300596	0.932111324	0.115210245	0.860918304	0
9638	0.260851	0.933853832	0.127305377	0.873249401	1
32667	0.299253	0.959811786	0.091914368	0.867089627	0
34750	0.304575	0.951999122	0.099191053	0.863451239	0
21092	0.31617	0.936177946	0.108731471	0.858249425	0
28889	0.327915	0.949214444	0.09618857	0.856598872	0
18964	0.303315	0.938694965	0.110899929	0.861114411	0
9301	0.273335	0.927134808	0.1276279	0.873631998	1
28758	0.362864	0.944921501	0.091267655	0.842319056	0
8521	0.269922	0.932088982	0.125012336	0.872845918	1
9475	0.274166	0.916474163	0.147605483	0.868018733	1
14917	0.279434	0.926004474	0.128673513	0.867805913	0
25961	0.340012	0.949237017	0.090816972	0.861026881	0
22105	0.346957	0.926848875	0.108737955	0.846607098	0

CONCLUSION

Biomedical image processing requires an integrated knowledge in mathematics, statistics, programming and Biology. The values obtained are essential as they represent the image and are necessary in order to classify the images accurately. Based on the result of the classifier, this project has a sensitivity of 80% and specificity of 20%. It is able to achieve a fairly accurate classification for mild and higher stages, but not for normal class resulting in a possible high false alarm. This might be improved by fine tuning the threshold values used on the images and more images could be used to improve the overall system. In this paper, we learnt various techniques of image processing and were able to extract the features namely blood vessels, exudates and micro aneurysms and texture properties like area, energy, contrast, correlation and homogeneity from the fundus images.

CONFLICT OF INTEREST
There is no conflict of interest.

ACKNOWLEDGEMENTS
None

FINANCIAL DISCLOSURE
None.

REFERENCES

- [1] CJ Vyborny, ML Giger, and RM Nishikawa. [2000] Computer aided detection and diagnosis of breast cancer," *Radiologic Clinics N. Amer.*, 38(4):725-740, 10.1016/S0033-8389(05)70197-4, 0033-8389.
- [2] J Scharcanski and CR Jung, [2006] Denoising and enhancing digital mammographic-Images for visual screening, *Computerized Medical Image, Graphics*, 30 (4):243-254, 10.1016/j. comp med image, 2006.05.002, 0895-6111.
- [3] AntoBennet, M, Sankar Babu G, Natarajan S, [2015] Reverse Room Techniques for Irreversible Data Hiding, *Journal of Chemical and Pharmaceutical Sciences* 08(03): 469-475.
- [4] AntoBennet M, Sankaranarayanan S, Sankar Babu G,[2015] Performance & Analysis of Effective Iris Recognition System Using Independent Component Analysis, *Journal of Chemical and Pharmaceutical Sciences* 08(03): 571-576.
- [5] Dr. AntoBennet, M, Suresh R, Mohamed Sulaiman S,[2015] Performance & analysis of automated removal of head movement artifacts in EEG using brain computer interface", *Journal of Chemical and Pharmaceutical Research* 07(08): 291-299.
- [6] AntoBennet, M & JacobRaglend, [2012] Performance Analysis Of Filtering Schedule Using Deblocking Filter For The Reduction Of Block Artifacts From MPEQ Compressed Document Images, *Journal of Computer Science*, 08(09): 1447-1454.
- [7] AntoBennet, M & JacobRaglend, [2001] Performance Analysis of Block Artifact Reduction Scheme Using Pseudo Random Noise Mask Filtering, *European Journal of Scientific Research*, 66(01): 120-129.
- [8] AntoBennet M, Resmi R Nair, Mahalakshmi V, Janakiraman G [2016] Performance and Analysis of Ground-Glass Pattern Detection in Lung Disease based on High-Resolution Computed Tomography, *Indian Journal of Science and Technology*, 09(02):01-07.
- [9] AntoBennet M & JacobRaglend. [2012] A Novel Method Of Reduction Of Blocking Artifact Using Machine Learning Metric approach, *Journal of Applied Sciences Research*,8(05): 2429-2438.